









## Research Article

# Forecasting Ionospheric TEC Changes Associated with the December 2019 and June 2020 Solar Eclipses: A Comparative Analysis of OKSM, FFNN, and DeepAR Models

R. Mukesh <sup>1</sup>, Sarat C. Dass <sup>2</sup>, Negash Lemma Gurmu <sup>3</sup>, M. Vijay <sup>1</sup>, S. Kiruthiga <sup>4</sup>, S. Mythili <sup>5</sup>, D. Venkata Ratnam <sup>6</sup>, and V. B. S. Srilatha Indira Dutt <sup>7</sup>

<sup>1</sup>Department of Aerospace Engineering, ACS College of Engineering, Bangalore, India

<sup>2</sup>School of Mathematical & Computer Sciences, Heriot-Watt University Malaysia, Putrajaya, Malaysia

<sup>3</sup>Department of Industrial Engineering, Ambo University, Ambo, Oromia, Ethiopia

<sup>4</sup>Department of ECE, Saranathan College of Engineering, Trichy, India

<sup>5</sup>Department of ECE, PSNA College of Engineering and Technology, Dindigul, India

<sup>6</sup>Department of ECE, KL University, Guntur, Andhra Pradesh, India

<sup>7</sup>Department of EECE, GITAM School of Technology, Visakhapatnam, India

Correspondence should be addressed to Negash Lemma Gurmu; [negash.lemma@ambou.edu.et](mailto:negash.lemma@ambou.edu.et)

Received 11 September 2023; Revised 28 November 2023; Accepted 12 March 2024; Published 19 March 2024

Academic Editor: Fernando Aguado Agelet

Copyright © 2024 R. Mukesh et al. This is an open access article distributed under the Creative Commons Attribution License, which permits unrestricted use, distribution, and reproduction in any medium, provided the original work is properly cited.

This paper presents forecast and investigation of the variation in ionospheric Total Electron Content (TEC) during the solar eclipses (SEs) of December 2019 and June 2020 using three different methods: Deep Autoregressive model (DeepAR), Feed-Forward Neural Network (FFNN), and Ordinary Kriging-based Surrogate Model (OKSM), and the TEC data predicted by DeepAR, FFNN, and OKSM were compared with the actual TEC during the observation days. The study was conducted based on GPS data taken from the IISC receiver located in Bangalore, India, during the SEs which happened on 26.12.2019 and 21.06.2020. The TEC data were examined to assess the effect of solar eclipses on TEC values. Eighty-day prior TEC data for the IISC station are gathered from IONOLAB servers along with the other parameter data like Dst, Ap, F10.7, and Kp taken from OMNIWEB servers which were used to predict TEC. The reliability of the forecasted results is evaluated using numerical factors like Normalized Root Mean Square Error (NRMSE), Correlation Coefficient (CC), Root Mean Square Error (RMSE), Mean Absolute Error (MAE), and R-squared. The study demonstrates the usefulness of combining multiple methods for analyzing TEC variations during SEs and highlights the potential of OKSM, FFNN, and DeepAR models for studying TEC variation in the same context. The findings may be useful for satellite broadcasting and navigational services and for further research into the influence of solar eclipses on the TEC changes.

## 1. Introduction

A solar eclipse appears while the Moon moves between the Earth and the Sun, which creates a shadow on the Earth. During SE, the Moon's shadow is routed across the surface of the Earth, creating a path of totality, where the Sun is completely blocked, and a partial eclipse, where the Sun is only partially obscured. The path of totality is relatively

narrow, and only those in the direct path are able to witness the full eclipse. However, even those outside the path of totality can witness a partial eclipse. In recent times, SEs have become a subject of scientific study and observation. Astronomers and researchers use SEs to study the Sun's corona (Sun's outer layer), which is normally obscured by the brightness of the Sun. The impact of SE on the Earth's ionosphere and satellite signal is given in Figure 1.

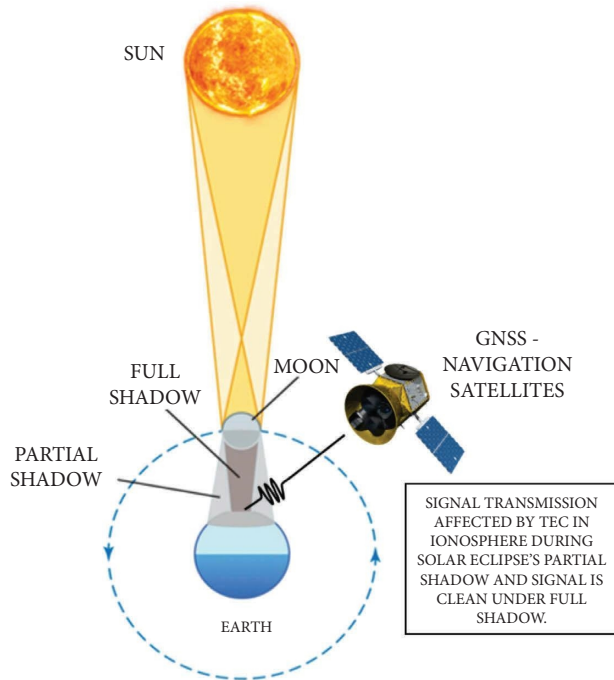


FIGURE 1: GNSS signal variation during solar eclipse.

The ionospheric TEC changes during the solar eclipses were examined by very few studies; some of them are briefly discussed below. Li et al. [1] analyzed the monthly, daily, and seasonal change of TEC based on the data taken from the BJFS situated in China. IRI 2012 TEC data were correlated with the true TEC values. The results indicate that the IRI model underestimates the TEC during night-time, but the model performs well during the daytime, especially during the low solar activity year. Swiatek and Stanislawski [2] used data from two GPS receivers located at Warsaw and Borowiec. They also considered the Warsaw Ionosonde data to analyze the TEC variations during SE that occurred on 11.08.1999. Along with the GPS data, the IRI data were also used for TEC calculation, which was used for the updation of IRI models during solar eclipse. In another research, TEC variations on 21.6.2020 SE were analyzed according to the data taken from 6 GPS stations available in the regions of China and Taiwan. The outcome shows that during eclipse day, the TEC values were decreased at all the selected station areas [3]. The June 21, 2020, solar eclipse effects of ionospheric TEC variations were analyzed based on the data observed from 11 IGS network GPS data. Wavelet transform techniques were used for analyzing the results [4]. Chakraborty et al. [5] did investigation on the D region ionospheric TEC variations over India during the SE that occurred on 22.7.2009. They used the ion chemistry model to analyze the ion density and found that their model performed well. Kundu et al. [6] analyzed the ionospheric plasma variations at various altitudes during the SE and non-eclipse days based on the space and ground-oriented instruments. GUUG, CNMR, IISC, and HYDE IGS stations were chosen for this study. It is found that electron density decreases when the altitude increases, and the TEC data

reduced to 20–40% during the SE. Chen et al. [7] did an extensive analysis on the TEC changes in the August 2017 SE happened over the North America region based on a 3D tomography algorithm. The results show that 40% electron density depletion occurred as compared to the previous day. Chen et al. [8] used the TIEGCM model to investigate the reaction of the ionosphere during the 21.8.2017 SE and found that electron density decreased by 4TECU as compared to the normal quiet day. Amalia et al. [9] analyzed the 2017 SE effects on ionospheric TEC variations over North America with the help of GNSS and geomagnetic data. The TEC values during the SE were fed into the Chapman model to predict the magnetic field components and it was found to be matching well. Prabhakar et al. [10] analyzed the ionospheric E layer variations during July 2009 SE over the Indian region. They found that  $f^oF_2$  values fluctuated and remained at increased levels for a long duration during the total SE hours. The 1997 SE influence on the ionosphere over Irkutsk was analyzed using the data obtained from the GPS interferometer. The results show that the TEC depletion varies from 10 to 50% and is independent of longitude and latitude [11]. A neural network model was constructed to forecast the TEC during equinoxes and solstices by using the data taken from 3 South African stations. The predicted results were validated with IRI 2001 model, and it was found that the IRI model was not performing well [12]. Surabhi et al. [13] predicted the daily and seasonal TEC using Neural Networks with the help of data obtained from Bhopal GNSS receiver station. IRI 2016 model was used for validation, and it was found that NN model predicts well. In a recent research, LSTM neural network model was developed to forecast the spherical harmonic coefficients during storm and quiet days. The developed model results were collated with the IRI and NeQuick-2 models and it shows that the observed LSTM model produces reliable results [14]. Reddybattula et al. [15] developed a deep learning model to forecast the TEC during the 24<sup>th</sup> solar cycle based on data from the low latitude IISC station. The predicted TEC data were justified with the IRI 2016 model and it was found that the deep learning model results closely matched the true TEC values. Iban and Senturk [16] applied regression, random forest, and support vector machine models to forecast the  $f^oF_2$ ,  $h^mF_2$ , and TEC values using data collected from digisondes and IGS stations during the period from 01.01.2012 to 31.12.2013. The results show that random forest model performs better. Chakrabarti et al. [17] studied the variations of TEC during the total SE that occurred on 21.8.2017 over North America based on the data obtained from the YADA and K5TD stations. Apart from that they also analyzed the C class solar flare effects on TEC during the SE and found that K5TD station data show the effect of solar flare, but the YADA station data did not show the TEC variations because the solar flare affected area was available behind the lunar disk. After a complete study of the aforesaid literature, this research tries to forecast and investigate the ionospheric TEC changes during 2019 and 2020 SEs that appeared over the Indian region.

## 2. Methodology

The methodology used in the study is given in Figure 2. The study was conducted using GPS data observed from the IISC station in Bangalore, India (latitude: 13.0198°N; longitude: 77.5661°E). The TEC data were forecasted and examined to assess the effect of SEs on ionospheric anomalies. The SE occurred on 26.12.2019 and 21.06.2020. Three different models, namely, OKSM, which is an interpolation technique, FFNN, and DeepAR, which are based on Artificial Intelligence, are used in this research to predict TEC during 2019/2020 SEs. All the models utilize TEC data collected from IONOLAB servers (<https://www.ionolab.org>) along with solar parameters obtained from OMNIWEB servers (<https://omniweb.gsfc.nasa.gov>).

In this paper, the constructed surrogate model (OKSM) utilizes the preceding six days of TEC along with other data such as Disturbance storm time index (Dst), Planetary K index (Kp), Radio Flux at 10.7 cm (F10.7), and Planetary A index (Ap) to forecast the next day TEC. The Kp index is a value of the global geomagnetic activity level over a 3-hour period. Generally, higher Kp values are associated with increased ionospheric disturbances. The Ap index is a daily averaged planetary geomagnetic activity index derived from Kp values measured at 13 geomagnetic observatories worldwide. It provides a long-term view of geomagnetic activity compared to the Kp index. Elevated Ap values are indicative of increased ionospheric disturbances, affecting TEC accordingly. The F10.7 index denotes solar radio flux at a wavelength of 10.7 cm. The Dst index measures the globally averaged geomagnetic field disturbance caused by a geomagnetic storm. Geomagnetic storms, as indicated by the Dst index, can significantly impact the ionosphere. During a storm, TEC can experience both enhancements and depletions, depending on the storm's characteristics and the location in the ionosphere. Space weather indices such as Dst, Kp, F10.7, and Ap are critical for monitoring and predicting ionospheric variations. Hence, we have considered those solar and geomagnetic parameters as input to our model along with the true TEC values for TEC prediction. The basic TEC forecast procedure adopted by OKSM is given in the following equation [18, 19]:

$$\hat{f}(x_p) = \sum_{i=1}^N \gamma_i(x_i) f(x_i). \quad (1)$$

The FFNN models use the previous seventy-nine days of training data to forecast the next day's TEC. The predicted data are further validated with the one-day testing data. The FFNN model utilized in this paper is given in Figure 3 [20]. A FFNN is a simple form of neural networks. In FFNN, the flow of information proceeds in the forward direction and the model functionalities are given in (2) and (3) [21].

$$E_D = \frac{1}{2} \sum_{i=1}^N (\text{TEC}_{\text{true}}^i - \text{TEC}_{\text{pred}}^i)^2, \quad (2)$$

where  $\text{TEC}_{\text{true}}^i$  and  $\text{TEC}_{\text{pred}}^i$  are true and predicted TEC.

$$J(w) = \alpha E_w + \beta E_D, \quad (3)$$

$$E_w = \frac{1}{2} \sum_i^n w_i^2 \text{ is the weight decay,}$$

where  $J(w)$  represents the Bayesian parameter,  $\alpha$  and  $\beta$  are hyperparameters, and  $E_D$  represents the sum of squares of error.

DeepAR is a supervised ML approach which can be utilized for probabilistic forecasting. The DeepAR approach is constructed using Autoregressive Recurrent Neural Networks. The model is driven by a signal  $x(t)$  which is specified by (4). The RNN component uses this equation to model hidden layers. The DeepAR uses (5) to compute the training data. The parameter  $y$  is applied by a multilayer recurrent neural network with RNN cells parameterized by  $\Theta$  [22]. The DeepAR model uses previous seventy-nine days of input data such as TEC, F10.7, SSN, Kp, and Ap. The model is trained on a dataset comprising seventy-nine days of TEC data and the eightieth day testing data reserved for validation with the predicted data.

$$y^{(t)} = f(y^{(t-1)}, x^{(t)}; \theta), \quad (4)$$

$$y_{i,t} = h(y_{i,j-1}, z_{i,j-1}, x_{i,j}; \theta), \quad (5)$$

where  $y^{(t)}$  represents the system state and  $\theta$  represents the transit function parameter.

Traditionally, for deep learning methods, the training and test data are chosen as 70–30% or 80–20%, depending on the applications (Senturk et al. [23] and Saqib et al. [24]). But in this research, since the DeepAR and FFNN models are compared with OKSM and to have a similarity of comparison, the prediction interval of the AI/ML models is developed in such a way that it utilizes seventy-nine days of data to predict the next day TEC. Our goal is to measure and demonstrate the accuracy of the model for a day ahead TEC value prediction. To evaluate the precision of the model, we need to have certain points which are not used in the model training process and those kinds of set of points will be predicted by the trained model and it will be compared with the set of testing points which was not used for training.

## 3. Results and Discussion

Performance assessment estimation of the forecasted TEC was done by using five metrics like, CC, RMSE, MAE, NRMSE, and  $R$ -squared. The arithmetic forms of the statistical parameters are given in equations (6)–(10).

The comparison results of three models, DeepAR, FFNN, and OKSM, during the 2019 SE are provided in Table 1. The results indicate that OKSM acts better when compared with DeepAR and FFNN in terms of all metrics, especially MAE, where OKSM shows the lowest error. The average RMSE, CC, and NRMSE of OKSM are 1.38, 0.9833, and 1.06, respectively, which are better than those of DeepAR and FFNN. The comparison results of three models during the

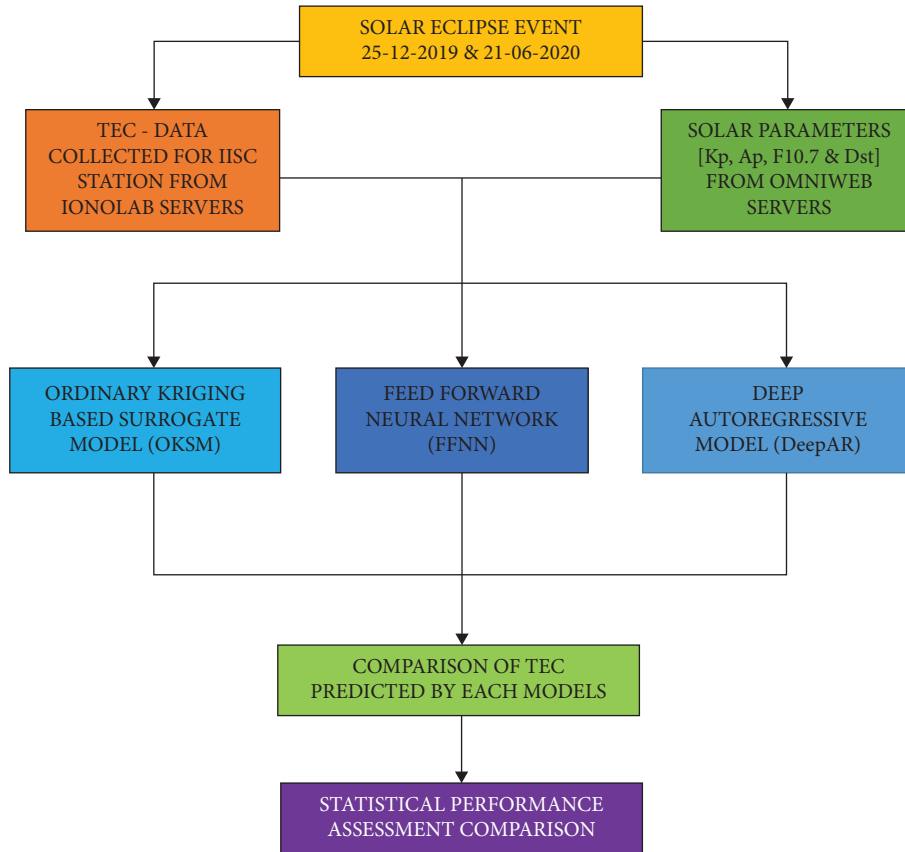


FIGURE 2: Methodology used in this research.

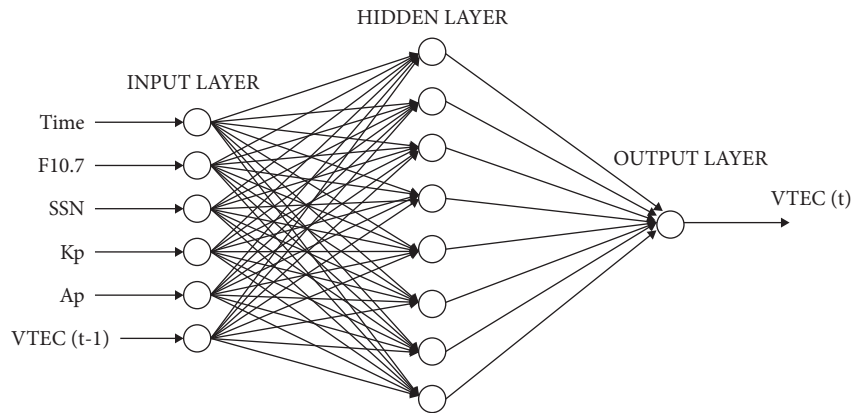


FIGURE 3: FFNN framework used in the research.

2020 SE are given in Table 2. Table 2 results show that, on average, OKSM and FFNN have similar performance, while DeepAR has a slightly higher RMSE, MAE, and NRMSE but a similar CC and R-squared. Additionally, the results imply that the performance of all three methods changes across

different dates during the SE. For example, on some dates, OKSM outperforms the other two methods, while on other dates, FFNN performs better. Moreover, DeepAR has a higher RMSE, MAE, and NRMSE than the other two methods on most dates.

$$\text{RMSE} = \sqrt{\frac{1}{N} \sum_{i=1}^N (\text{TEC}_{\text{TRUE}} - \text{TEC}_{\text{PRED}})^2}, \quad (6)$$

$$\text{NRMSE} = \frac{\text{RMSE}}{\text{MEAN of TRUE TEC}}, \quad (7)$$

$$\text{MAE} = \frac{\sum_{i=1}^N \text{abs}(\text{TEC}_{\text{TRUE}} - \text{TEC}_{\text{PRED}})}{N}, \quad (8)$$

$$\text{CC} = \frac{\sum_{I=1}^N (\text{TEC}_{\text{TRUE}} - \overline{\text{TEC}_{\text{TRUE}}}) (\text{TEC}_{\text{PRED}} - \overline{\text{TEC}_{\text{PRED}}})}{\sqrt{\sum_{I=1}^N (\text{TEC}_{\text{TRUE}} - \overline{\text{TEC}_{\text{TRUE}}})^2 \sum_{I=1}^N (\text{TEC}_{\text{PRED}} - \overline{\text{TEC}_{\text{PRED}}})^2}}, \quad (9)$$

where  $\overline{\text{TEC}_{\text{TRUE}}}$  and  $\overline{\text{TEC}_{\text{PRED}}}$  represent mean values of true and predicted TEC.

$$\text{RSQUARED} (\mathbf{R}^2) = 1 - \frac{\text{SUM OF RESIDUAL SQUARES}}{\text{TOTAL SUM OF SQUARES}}. \quad (10)$$

**3.1. Forecast of TEC during 2019 Solar Eclipse.** Figures 4 and 5 represent true TEC values and other parameters considered in this research. The data are obtained on an hourly basis in a continuous plot format from 21-11-2019 to 31-12-2019. The data are structured as 24 observation points per day, indicating that hourly readings were taken over the course of the twenty-day period. The plot is constructed as a five-layer stacked plot. The 5 layers named from the bottom to the top represent Kp, Dst, Ap, F10.7, and true TEC.

Figure 6 shows the comparison between previous five-day median TEC values and TEC on 26-12-2019 (eclipse day). The vertical lines in Figure 7 show the time interval of the eclipse on the observed date. From Figure 7, it is spotted that during the eclipse period, the TEC values show a large TEC depletion during that period. The maximum depletion during that maximum eclipse period is measured as 5.0964 TECU (31.4%) and this reduction in TEC is due to the Moon's obscuration of Sun's disk.

Table 3 shows the TEC difference observed extent in the IISC GPS station affected by solar eclipses. The difference in TEC values was obtained by comparing the previous five-day median TEC values with the TEC estimated during the SE days. It is seen that during the eclipse event, the TEC depletion % measured at the maximum eclipse time is 31.4% and 0.99% for the 2019 and 2020 eclipse, respectively. TEC depletion and TEC depletion % are calculated using (11) and (12).

$$\text{dTEC} = \text{TEC}_{\text{observed}} - \text{TEC}_{\text{median}} \quad (11)$$

$$\text{dTEC \%} = \frac{(\text{TEC}_{\text{observed}} - \text{TEC}_{\text{median}})}{\text{TEC}_{\text{median}}} \times 100, \quad (12)$$

where dTEC is the difference in TEC at that particular time period.

Since the ionospheric environments during the eclipse are generally not influenced by geomagnetic and solar activities, both the observed TEC on the eclipse day and the previous 5-day median TEC values did not exhibit any space weather effects capable of altering the ionosphere's permanent variations. This leads to a robust argument asserting that the changes in the ionosphere are directly associated with the SE [25]. The 2019 eclipse taken for observation occurred during the winter solstice and the 2020 eclipse occurred during the summer solstice. The solar eclipse happened on 26-12-2019 which was four days after the winter solstice. During the winter season eclipse, the TEC variation ranged from 3.09 to 20.13 TECU. Similarly, the solar eclipse happened on 21-06-2020 and on the same day itself the summer solstice also occurred. During the summer season eclipse, the TEC variation ranged from 0.15 to 18.33 TECU. It is notable that during both the solar eclipse periods, the TEC values have been reduced considerably when compared to the previous 5 days median value during both day and night times. The solstice can influence some of the input parameters, but it is notable that these changes are not directly caused by the solstice itself. It is important to consider that these parameters are influenced by various solar and space weather phenomena that may not have a direct correlation with the Earth's location in its orbit during the solstices.

During a total SE, the Moon moves between the Sun and the Earth, causing the Sun to be completely obscured for a less period of time. This astronomical event leads to a substantial decrease in solar radiation influencing the Earth's surface. The reduced solar radiation decreases the ionization in ionosphere which contains a concentration of ions and free electrons. When a total SE occurs, the direct solar radiation that normally ionizes the ionosphere is blocked by the Moon. As a result, the ionization process decreases, leading to a temporary reduction in the concentration of ions and free electrons available in the ionosphere. This decrease in ionization can have various effects on radio wave propagation, communication systems, and global navigation satellite systems. The reduction in ionization during a solar eclipse can introduce dynamic changes in the Earth's ionosphere, influencing radio wave

TABLE 1: Performance assessment comparison of OKSM, FFNN, and DeepAR during the 2019 solar eclipse.

Date	RMSE			CC			MAE			NRMSE			R-squared		
	OKSM	FFNN	DeepAR	OKSM	FFNN	DeepAR	OKSM	FFNN	DeepAR	OKSM	FFNN	DeepAR	OKSM	FFNN	DeepAR
22-12-2019	1.66	1.44	2.08	0.9837	0.9723	0.9888	1.34	1.10	1.68	0.15	0.13	0.19	0.9171	0.9375	0.8704
23-12-2019	1.35	2.24	1.91	0.9794	0.9645	0.9617	0.91	1.49	1.27	0.12	0.20	0.17	0.9589	0.8869	0.9180
24-12-2019	1.20	0.91	1.97	0.9849	0.9926	0.9631	1.00	0.73	1.33	0.11	0.09	0.18	0.9675	0.9814	0.9127
25-12-2019	1.11	1.25	0.80	0.9930	0.9823	0.9936	0.92	0.95	0.70	0.11	0.12	0.08	0.9718	0.9643	0.9853
26-12-2019	1.40	1.96	2.15	0.9822	0.9497	0.9332	1.05	1.44	1.61	0.14	0.19	0.21	0.9449	0.8925	0.8703
27-12-2019	1.54	2.09	2.37	0.9696	0.9420	0.9448	1.12	1.45	1.51	0.15	0.20	0.22	0.9360	0.8810	0.8481
28-12-2019	1.42	1.91	2.74	0.9905	0.9927	0.9622	1.08	1.46	2.07	0.13	0.17	0.25	0.9595	0.9267	0.8497
Average	1.38	1.69	2.00	0.9833	0.9709	0.9639	1.06	1.23	1.45	0.13	0.16	0.19	0.9508	0.9243	0.8935

TABLE 2: Performance assessment comparison of OKSM, FFNN, and DeepAR during the 2020 solar eclipse.

Date	RMSE			CC			MAE			NRMSE			R-squared		
	OKSM	FFNN	DeepAR	OKSM	FFNN	DeepAR	OKSM	FFNN	DeepAR	OKSM	FFNN	DeepAR	OKSM	FFNN	DeepAR
18-06-2020	0.74	1.03	1.25	0.9952	0.9928	0.9877	0.52	0.78	0.96	0.08	0.11	0.14	0.9883	0.9773	0.9682
19-06-2020	1.20	1.32	1.33	0.9907	0.9922	0.9963	0.92	1.06	1.01	0.12	0.14	0.15	0.9744	0.9689	0.9570
20-06-2020	1.01	1.04	1.91	0.9912	0.9913	0.9659	0.67	0.80	1.41	0.11	0.11	0.22	0.9802	0.9788	0.9245
21-06-2020	0.97	1.19	1.57	0.9896	0.9851	0.9882	0.75	0.95	1.29	0.10	0.13	0.17	0.9786	0.9678	0.9589
22-06-2020	1.52	1.05	1.57	0.9767	0.9904	0.9797	1.04	0.79	1.01	0.16	0.11	0.16	0.9539	0.9779	0.9553
23-06-2020	1.75	2.06	2.13	0.9921	0.9920	0.9920	1.46	1.88	1.67	0.22	0.25	0.22	0.9276	0.9001	0.9218
24-06-2020	2.14	1.76	1.88	0.9617	0.9690	0.9781	1.80	1.44	1.59	0.22	0.18	0.22	0.8798	0.9195	0.9249
Average	1.33	1.35	1.66	0.9853	0.9876	0.9840	1.02	1.10	1.28	0.14	0.15	0.18	0.9547	0.9558	0.9444

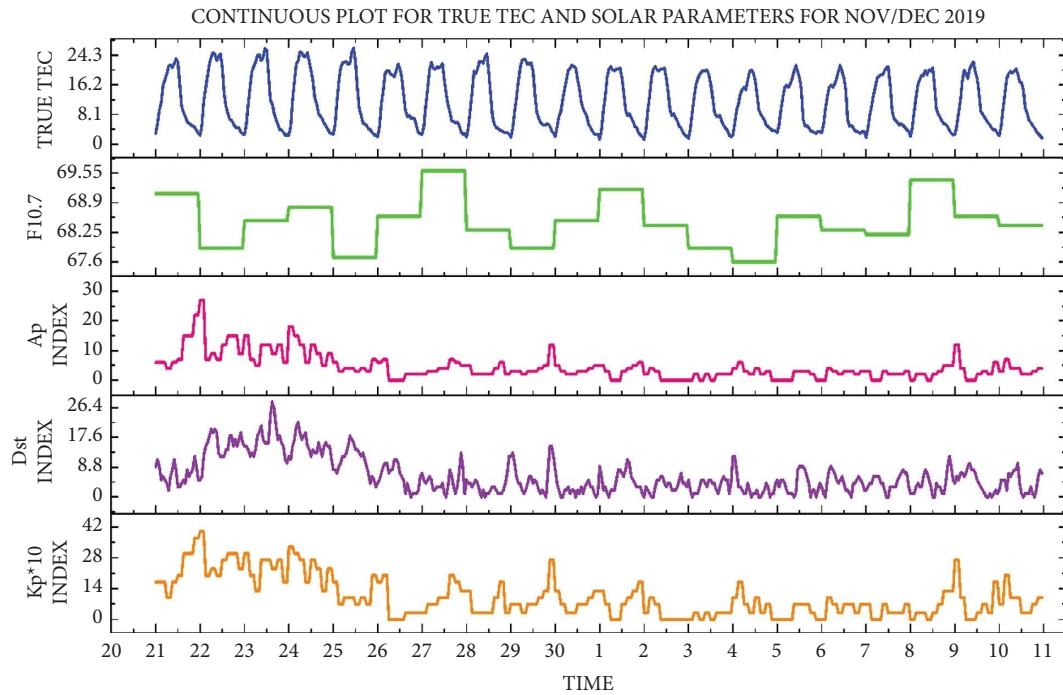


FIGURE 4: TEC and solar parameters from 21-11-2019 to 10-12-2019.

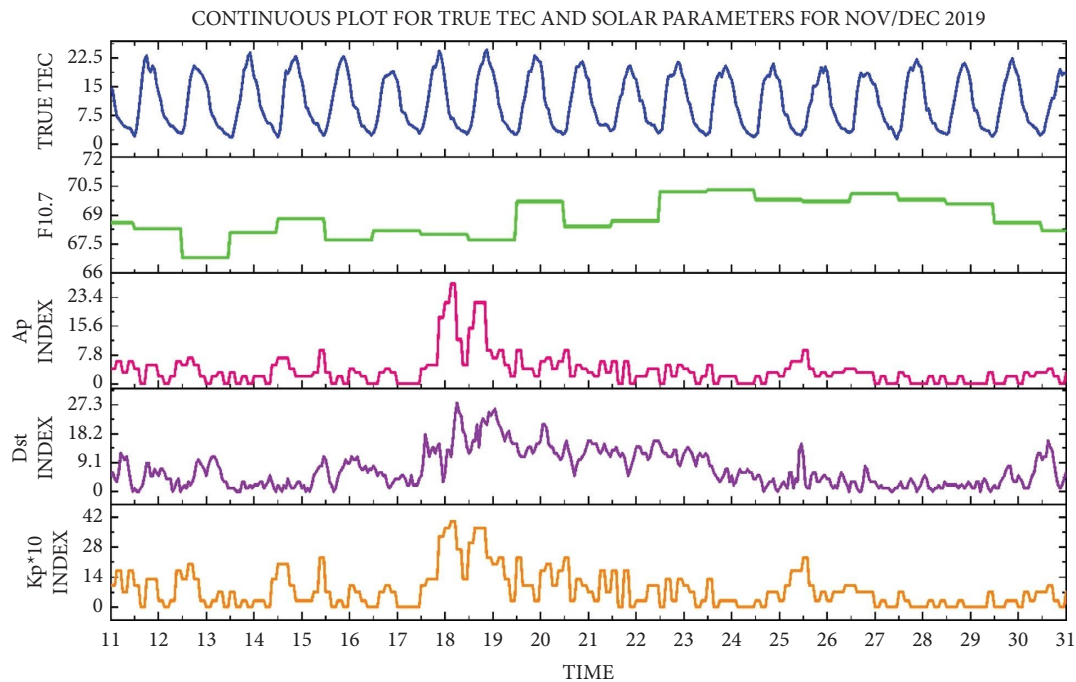


FIGURE 5: TEC and solar parameters from 11-12-2019 to 31-12-2019.

propagation, communication systems, and global navigation satellite systems. These negative effects may manifest as alterations in signal strength, signal delays, and disruptions in communication and navigation signals, presenting challenges for precise and reliable operations. However, these changes also offer valuable opportunities for scientific study and observation, providing insights into the

ionospheric response to celestial events and contributing to our understanding of space weather dynamics. The solar eclipse of 2019 marked an annular event with its central path traversing the Saudi Arabian Peninsula, Sumatra, India, Borneo, Guam, and the Philippines. The eclipse had a magnitude of 0.96, spanning 164 km in width and advancing eastward at an average speed of 1.1 km per second. It



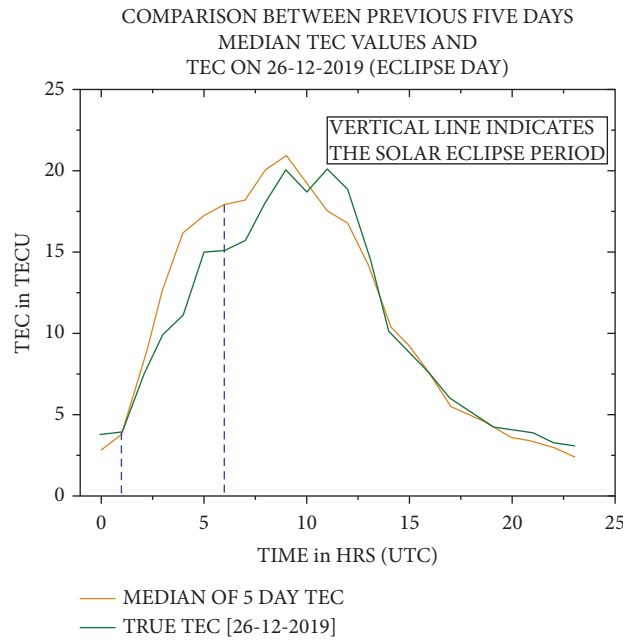


FIGURE 6: Comparison between previous five-day median TEC values and TEC on 26-12-2019 (eclipse day).

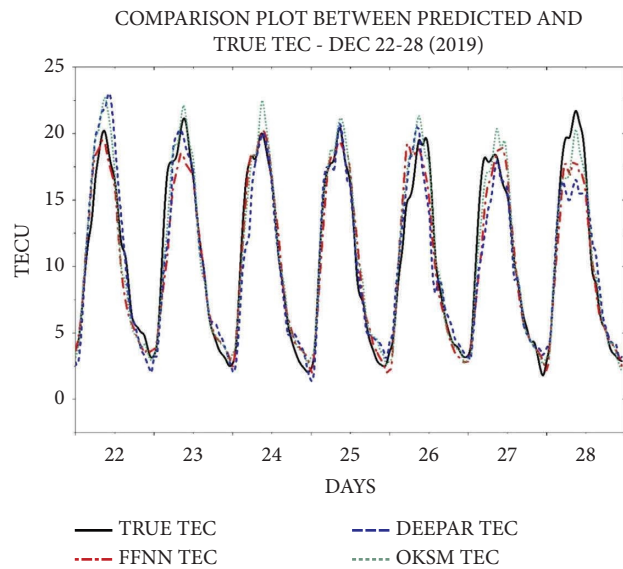


FIGURE 7: Comparison TEC plot of TRUE vs DeepAR, FFNN, and OKSM (2019).

TABLE 3: TEC depletion observed extent in the IISC GPS station affected by solar eclipses.

Eclipse date	Time of eclipse in India (UTC)	TEC depletion (TECU)	TEC depletion (%)
26-12-2019	04:27	5.0964	31.4
21-06-2020	02:33	0.1247	0.99

made its way to India, near Kannur, Kerala, casting its shadow over the southeast coast of India. The 2019 solar eclipse is an annular or partial eclipse which depends upon the location in India and for the considered IISC station, the SE had a maximum obscuration function of 89.4% [17]. The term obscuration function typically refers to the fraction of

the solar disk which was masked by the Moon during an eclipse. The obscuration function is a measure of how much of the solar disk is blocked by the Moon at a specific point in time during the eclipse. The effect of the obscuration function on ionospheric conditions can be significant. The obscuration function, representing the degree of solar disk

coverage, influences the amount of solar radiation affecting the Earth's atmosphere, which in turn affects the ionospheric TEC variations. Figure 7 shows the comparison diagram of true TEC and TEC predicted by DeepAR, FFNN, and OKSM. Figure 8 shows the comparison of TEC on the Annular Eclipse of 26.12.2019. The start of the partial eclipse over India occurred at 2:33 AM (UTC) followed by the start of annularity at 3:54 AM (UTC). The end of the annularity and the partial eclipse is recorded at 4:04 AM (UTC) and 6:42 AM (UTC), respectively. From Figure 8, we can see that the true TEC varies in an abrupt manner during the start of the eclipse as its values gradually increase with the progression of time. All three models captured the trend of TEC increase with slight variations of range at specific sample points. It is notable that the variation in the predicted TEC during the eclipse period is within 3 TECU. The true TEC values tend to be lowest during the early day hours (between 2:00 AM and 5:00 AM) and highest during the afternoon hours (between 12:00 PM and 5:00 PM). This suggests that TEC measurement is vastly affected by solar effects during different times of the day. The predicted TEC follows the same low-high-low pattern of TEC throughout the day. The values predicted are different for the three models considered. The TEC values predicted by DeepAR appear to be more stable over time, with relatively small fluctuations. The OKSM forecasted TEC data also seems to be relatively stable, with marginally high values in the midafternoon and evening hours indicating that the factors influencing this type of TEC measurement are consistent but may be slightly more pronounced during certain times of the day. Finally, the FFNN forecasted TEC data show a clear diurnal pattern, with the least values during early morning hours and the high values during the afternoon hours. This suggests that the factors that influence TEC values are strongly tied to the Sun's cycle. Upon examining forecasted TEC values by the DeepAR, FFNN, and OKSM models and comparing them with the true TEC values, it is evident that there are differences in their accuracy. The OKSM's TEC values are close to the actual TEC, with only minor variations. The FFNN TEC data are more distributed, revealing a higher degree of variability compared to the true TEC. In contrast, the DeepAR model's TEC data are consistent with the true TEC values, exhibiting a similar pattern and amplitude.

**3.2. Regression Analysis for OKSM, FFNN, and DeepAR during 2019 Solar Eclipse.** A linear regression plot would show a scatterplot of the true values vs the predicted values with a line of best fit over the data. A linear regression plot can give valuable insights into the accuracy of a regression model's predictions and can help identify areas for improvement. Since the goal here is to see how well the forecasted TEC data match the true ones, the fitted linear regression model should ideally be close to the identity function, that is, with slope one and intercept zero. The performance assessment of the models used in this research using linear regression for the 2019 solar eclipse event is provided in Table 4. From the comparison of true and forecasted TEC values plotted as linear regression scatter

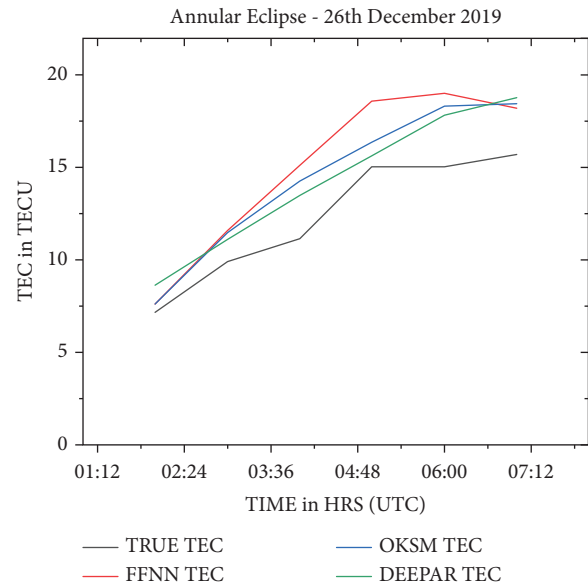


FIGURE 8: Comparison TEC plot of TRUE vs DeepAR, FFNN, and OKSM during 2019 SE.

plots in Figures 9–11 during the 2019 SE event, the OKSM TEC data show a higher level of accurateness as compared to the other two models. This can be attributed to the model's ability to obtain the temporal dependencies and patterns in the data, allowing it to make more accurate predictions. On the other hand, the FFNN TEC values show a good correlation with the true TEC values, indicating that it is also a competent model for TEC prediction. However, the DeepAR model's TEC values show a high variability, suggesting that it may not be the most reliable model for TEC prediction.

On the eclipse day (26.12.2019), we can compare the actual TEC with the forecasted TEC data obtained from the three models: DeepAR, FFNN, and OKSM. By observing the difference between the true TEC data and the forecasted TEC values, we can see that at 00:00:00 UTC, the true TEC value was 23.46 TEC units, while the OKSM forecasted a value of 24.07 TEC units, resulting in a difference of 0.61 TEC units. Similarly, the FFNN model predicted a TEC value of 21.57 TEC units, which resulted in a difference of 1.89 TEC units from the true value. But, the DeepAR model predicted a TEC value of 24.78 TEC units, resulting in a difference of 1.32 TEC units from the true value. As we move through the day, the variation between the models increases. Therefore, it is vital to consider the performance of different models during the prediction of TEC values under different circumstances. For all the models, the difference between the forecasted and true data ranges from 0.036 to 4.346, indicating that the chosen models are appropriate for ionospheric TEC anomaly studies. Looking at the linear regression fit parameters of the three models in Table 4, we see that OKSM predictions gave rise to a linear regression line that is closest to the identity function compared to DeepAR and FFNN. Hence, OKSM seems to provide closer correlation when related to the other two approaches.

TABLE 4: Performance assessment using linear regression (2019).

Model	Intercept	Slope	Pearson's R	R <sup>2</sup>
OKSM	0.2941 ± 0.19	0.9891 ± 0.01	0.97575	0.95208
FFNN	0.6758 ± 0.24	0.9028 ± 0.01	0.96444	0.93015
DeepAR	0.8859 ± 0.29	0.8896 ± 0.02	0.94753	0.89782

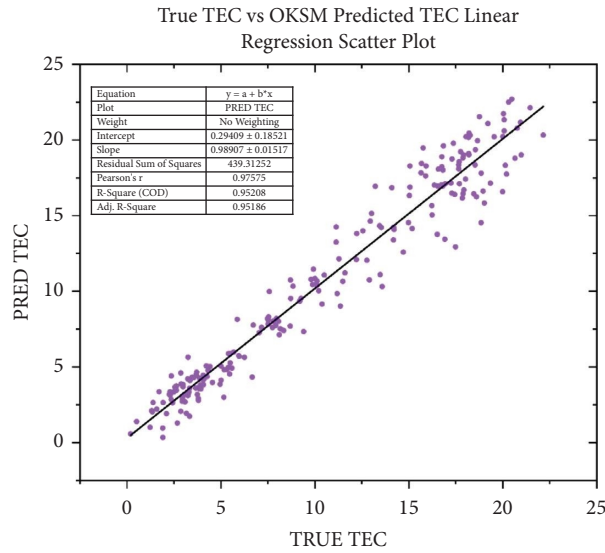


FIGURE 9: Linear regression scatter plot of TRUE vs OKSM predicted TEC (2019).

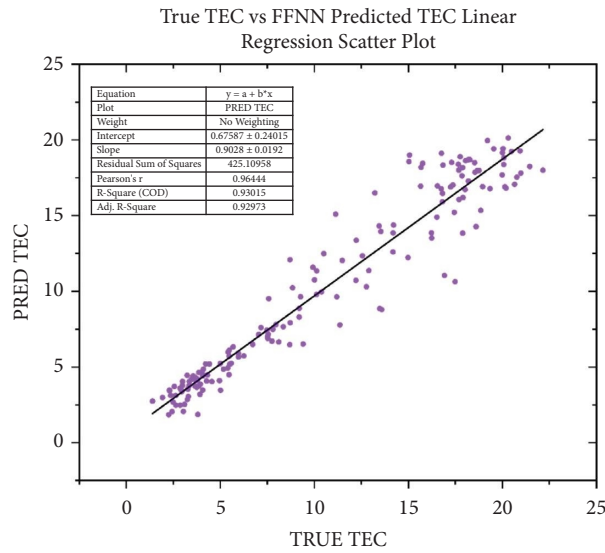


FIGURE 10: Linear regression scatter plot of TRUE vs FFNN predicted TEC (2019).

3.3. Forecast of TEC during 2020 Solar Eclipse. Figures 12 and 13 represent true TEC data along with the other parameters considered in this research on an hourly basis in continuous plot format from 22-5-2020 to 30-6-2020. The data are structured in 24 data points per day, indicating that hourly readings were taken over the course of the twenty-day

period. The plot is constructed as a five-layer stacked plot. Each layer from the bottom represents Kp, Dst, Ap, F10.7, and true TEC.

The trajectory of the 2020 annular eclipse spanned across portions of Central and Eastern Africa and the Southern Arabian Peninsula, encompassing Oman, Yemen, and

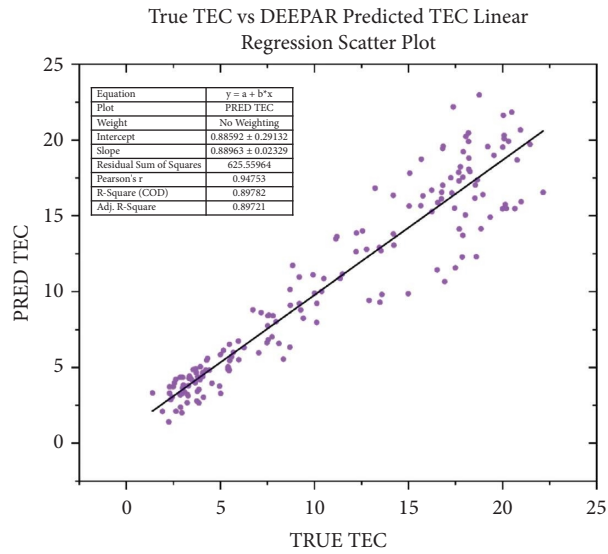


FIGURE 11: Linear regression scatter plot of TRUE vs DeepAR predicted TEC (2019).

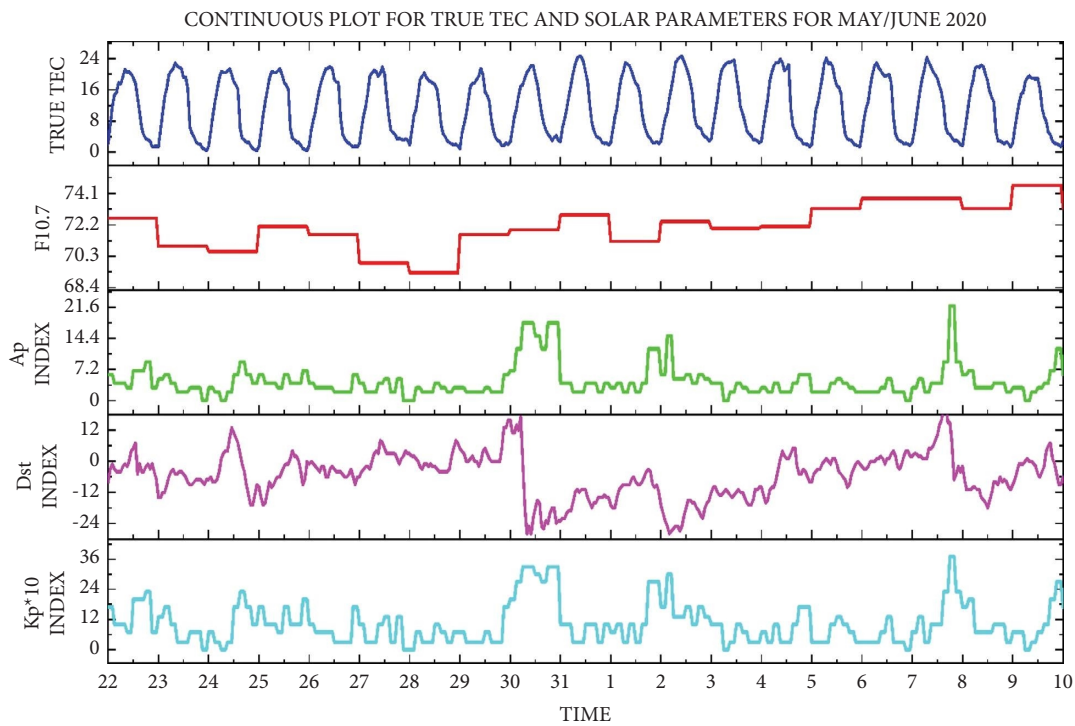


FIGURE 12: TEC and solar parameters from 22-5-2020 to 10-6-2020.

Southern Saudi Arabia. It extended through various regions, including Southern Pakistan, Northern India, and Nepal within South Asia and the Himalayas, as well as parts of East Asia, covering South China and Taiwan. Additionally, the path touched parts of Micronesia, specifically Guam. During the 2020 annular solar eclipse, the Moon was not able to fully cover the solar disk and the Sun looks like a bright ring. For the 2020 solar eclipse, the maximum obscuration is observed in India at Uttarakhand with a maximum obscuration of 98.6%, and over IISC, Bangalore, the obscuration function is

measured as 36.5%. Figure 14 shows a comparison between previous five-day median TEC values and TEC on 21-06-2020 (eclipse day). The vertical lines in Figure 15 show the time period of the eclipse on the observed date. From Figure 15, it can be seen that during the eclipse period, the TEC values show a small TEC depletion during that period. The maximum depletion during that maximum eclipse period is measured as 0.1247 TECU (0.99%) and this is due to the less obscuration function happened over the IISC station. Figure 15 shows the comparison plot between true

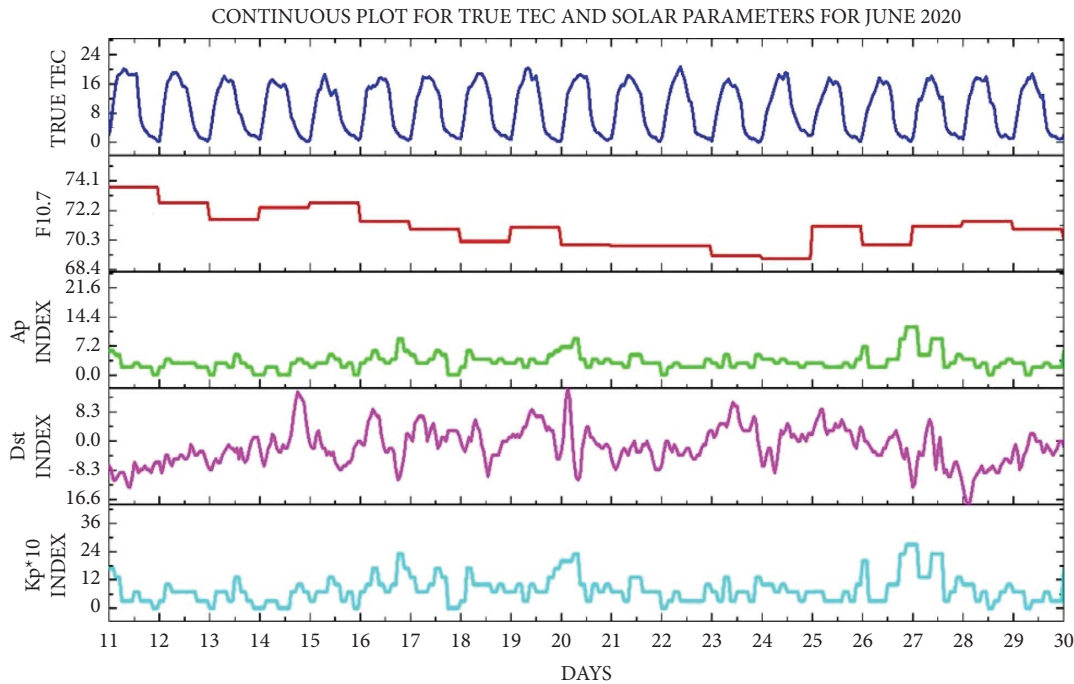


FIGURE 13: TEC and solar parameters from 11-6-2020 to 30-6-2020.

TEC and other three different predicted values for TEC. Figure 16 shows the comparison of TEC during the Annular Eclipse of June 21, 2020. The start of the partial eclipse over India occurred at 4:27 AM (UTC) followed by the start of annularity at 6:19 AM (UTC). The end of the annularity and the partial eclipse is recorded at 6:42 AM (UTC) and 9:02 AM (UTC), respectively. It is worth noting that while total solar eclipses do have measurable effects on ionization and TEC, these changes are temporary and typically return to their normal levels after the eclipse event has concluded and the Sun's radiation is once again reaching the Earth's ionosphere. From Figure 16, we can see that the true TEC during the 2020 SE is varying vastly in between the hours of 04:00 and 09:00 (UTC). All three models captured the variation of TEC at the initial hours but gradually deviated from the true TEC in the later part of the annularity. The maximum deviation of the models is measured up to 3 TECU which signifies the areas of improvement. The TRUE TEC value represents the actual TEC value measured on that particular date and time. Upon comparing the different predicted values with the TRUE TEC value, we can see that there is a variation in the time pattern of the predictions. Some predicted values are very close to the TRUE TEC value, while others are quite far off. However, it is significant to note that the accuracy of the predictions might vary and it depends on the particular time and date being studied. On the solar eclipse event date of June 21, 2020, the true TEC values are lower when compared with the dates prior and after the event. Out of the three models adapted in the research, the DeepAR model predicted a relatively high value, i.e., 22 TECU, on June 23, 2020. This is because all the

models are constructed based on sliding pattern and the true TEC on the previous day is significantly high TECU compared to the eclipse event date.

*3.4. Regression Analysis for OKSM, FFNN, and DeepAR during 2019 Solar Eclipse.* The performance assessment of the models used in this research using linear regression for the 2020 solar eclipse event is provided in Table 5. From the assessment of true and predicted values plotted as linear regression scatter plots in Figures 17–19 during the 2020 solar eclipse event, the OKSM forecasted TEC values show a higher level of accurateness compared to the other two models, FFNN and DeepAR. The OKSM's forecasted TEC values indicate that it is a competent model for TEC prediction. However, the FFNN and DeepAR model's forecasted TEC data show a high degree of residual, suggesting that it needs more attention for TEC prediction. On the eclipse event date of June 21, 2020, based on the predicted TEC values, we can see that the FFNN model consistently provides the highest predicted values, while the DeepAR model tends to provide the lowest predicted values. The OKSM model falls in between the two, but generally closer to the FFNN predictions. Looking at specific time intervals, we can see that the models provide different levels of accuracy at different times of day. For example, in the early morning hours (00:00–03:00), the DeepAR model is the most accurate, while the OKSM model consistently overpredicts the TEC values. In the early afternoon (10:00–14:00), the FFNN model provides the most accurate predictions, while the DeepAR model consistently underpredicts the TEC values. It

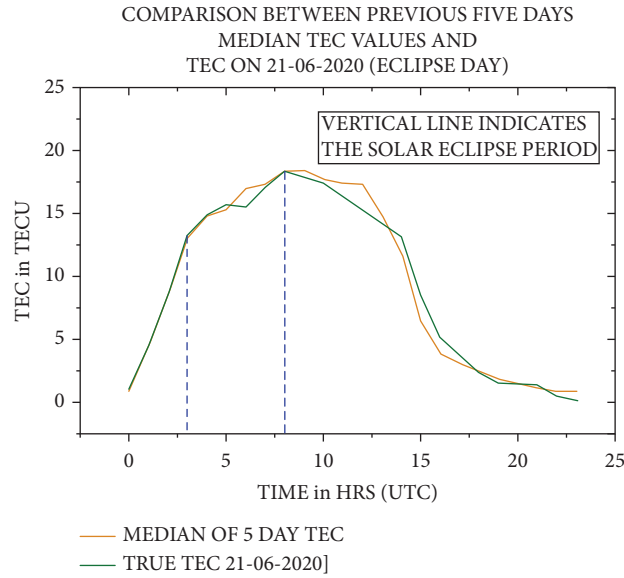


FIGURE 14: Comparison between previous five-day median TEC values and TEC on 21-06-2020 (eclipse day).

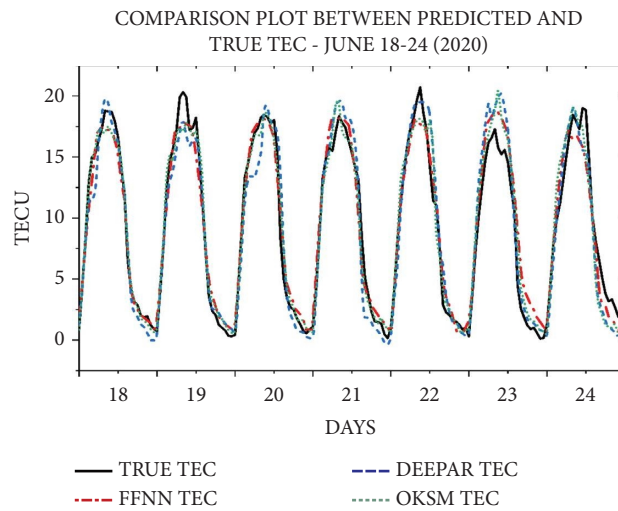


FIGURE 15: Comparison TEC plot of TRUE vs DeepAR, FFNN, and OKSM (2020).

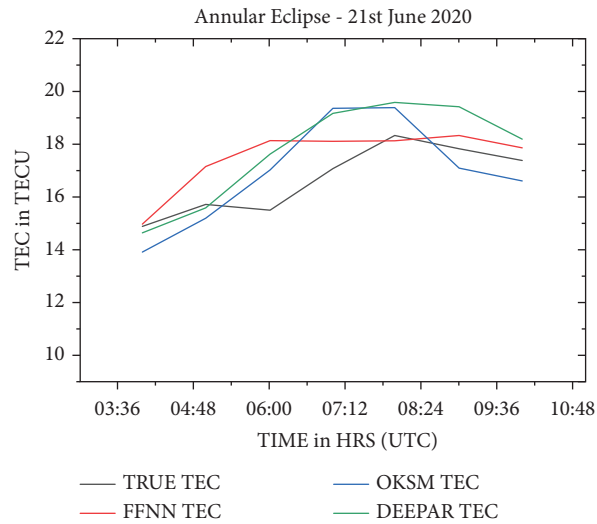


FIGURE 16: Comparison TEC plot of TRUE TEC vs DeepAR, FFNN, and OKSM during 2020 SE.

TABLE 5: Performance assessment using linear regression (2020).

Model	Intercept	Slope	Pearson's <i>R</i>	<i>R</i> <sup>2</sup>
OKSM	0.2973 ± 0.16	0.9773 ± 0.01	0.97695	0.95444
FFNN	0.6667 ± 0.14	0.9468 ± 0.01	0.98057	0.96151
DeepAR	-0.2548 ± 0.22	1.0153 ± 0.01	0.9721	0.94498

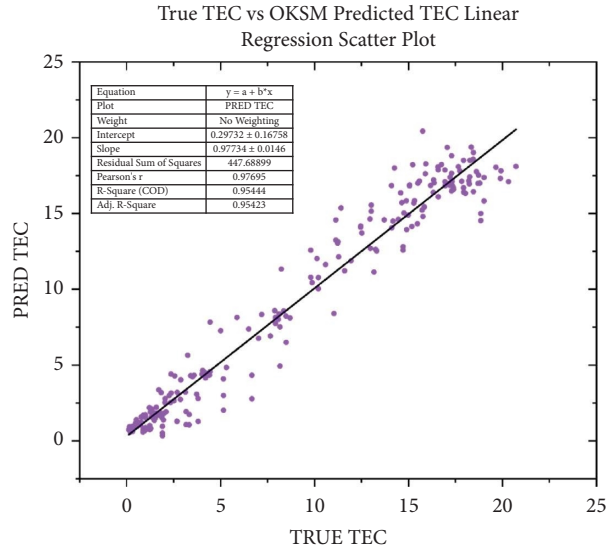


FIGURE 17: Linear regression scatter plot of TRUE vs OKSM predicted TEC (2020).

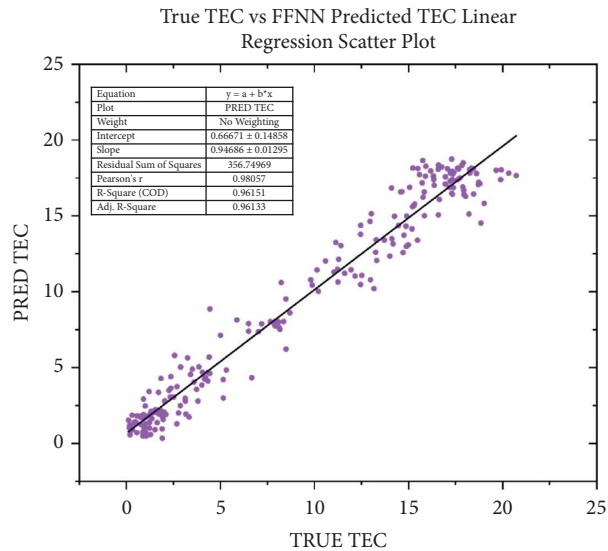


FIGURE 18: Linear regression scatter plot of TRUE vs FFNN predicted TEC (2020).

is clear that each model has its strengths and weaknesses, and the most accurate model will depend on the specific time and location being predicted. It is important to evaluate and compare the performance of multiple models to get a more comprehensive understanding of TEC predictions. The comparison of the predicted TEC values for June 21, 2020, reveals that the three models used, namely, OKSM, FFNN, and DeepAR, have varying levels of accuracy in predicting

TEC. Looking at the data, it is evident that the OKSM model has the best accuracy among the three models as it consistently predicted the TEC values closer to the true TEC throughout the day. On the other hand, the FFNN model appears to have the next best accuracy in forecasting TEC values for most hours of the day, although it slightly overpredicted the TEC values in the early morning hours. Meanwhile, the DeepAR model also showed good accuracy

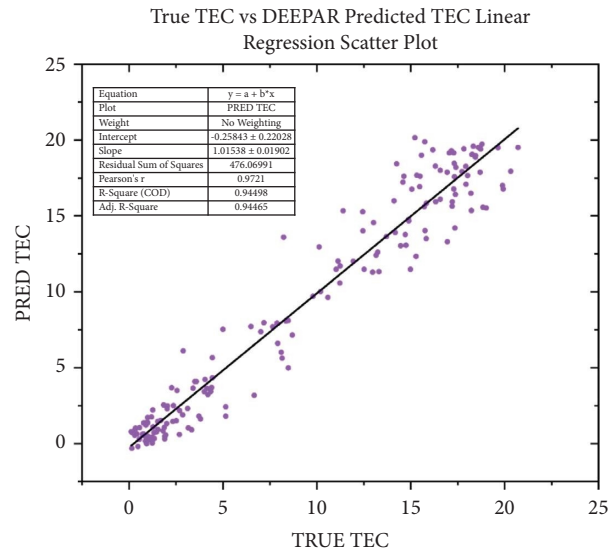


FIGURE 19: Linear regression scatter plot of TRUE vs DeepAR predicted TEC (2020).

in predicting TEC values, although it appears to be less accurate in the early morning hours than the FFNN model. Overall, the three models performed well in predicting TEC values, with each model showing a different level of accuracy depending on the time of day. It is important to note that comparing the accuracy of these models is just one aspect of evaluating their performance. Other factors such as the complication of the model, the computational cost, requirement of training data, and the ease of execution are also valuable considerations when choosing a model for a specific application. Table 5 indicates that OKSM and DeepAR provide the closest matches between true and predicted TEC values for this dataset.

#### 4. Conclusion

This research primarily focuses on predicting ionospheric TEC changes associated with the solar eclipses that occurred in December 2019 and June 2020. Three different models, namely, OKSM, FFNN, and DeepAR, are constructed to forecast TEC before and after the solar eclipse days over the IISC station, Bangalore, India. The OKSM is an interpolation method which uses 6 days of input data such as TEC and solar parameters to forecast the next day TEC, whereas the DeepAR and FFNN models are AI/ML-based techniques that use 79 days of input data to forecast the next day TEC data. The results of the three models are estimated using statistical parameters such as CC, RMSE, MAE, NRMSE, and R-squared. The research addresses the distinct strengths and adaptabilities of OKSM, FFNN, and DeepAR in response to annular solar eclipse scenarios.

Based on the results, it can be decided that during the 2019 SE, the OKSM generally performed well as compared with the FFNN and DeepAR models, as indicated by its lower RMSE, higher CC, and higher R-squared values, as well as the close match of the linear regression line. The MAE was lowest for the FFNN model. From the results, we can see that during the 2019 solar eclipse, the OKSM had the lowest

average RMSE of 1.38, followed by the FFNN model with an average RMSE of 1.69, and DeepAR with an average RMSE of 2.00. In terms of CC, which measures linear correlation between the forecasted and actual values, OKSM also had the highest average value of 0.9833, while DeepAR had the lowest average value of 0.9639. However, during the 2020 SE, the performance of the three models shows high diversity. While the OKSM still had the lowest RMSE and highest CC and R-squared values, the DeepAR model had the lowest MAE. The FFNN model had similar performance to the other models in terms of CC, RMSE, and R-squared values but had a little higher MAE than the other models on average. The results show that in the assessment comparison of the three models during the 2020 SE, the OKSM had a less average RMSE of 1.08, followed by FFNN with an average RMSE of 1.13, and DeepAR with an average RMSE of 1.44. In terms of CC, all three models had an approximate value of 0.98 with variation only in the third decimals. From the results, it is identified that the performance of the three models varied across the two SEs. The models were more reliable during 2019 and were more variable during the 2020 eclipse. These results suggest that the performance of different models varies based on the particular context and conditions in which they are used.

Overall, the results suggest that even with small datasets, OKSM gives more accurate results. With the availability of large volume of data, FFNN is the most effective model for predicting solar eclipse performance, while the DeepAR model is a competitive alternative.

#### Data Availability

All the datasets used for this work can be received upon request to the corresponding author.

#### Conflicts of Interest

The authors declare that they have no conflicts of interest.



## Acknowledgments

The research work presented in this paper has been carried out under the Project ID “VTU RGS/ DIS-ME/2021-22/ 5862/1,” funded by VTU, TEQIP, Belagavi, Karnataka.

## References

- [1] S. Li, L. Li, and J. Peng, “Variability of ionospheric TEC and the performance of the IRI-2012 model at the BJFS station, China,” *Acta Geophysica*, vol. 64, p. 1970, 2016.
- [2] A. Swiatek and I. Stanisławska, “Updating the local model of the TEC during the solar eclipse on August 11, 1999,” *Cosmic Research*, vol. 41, no. 4, pp. 315–318, 2003.
- [3] S. S. Rao, M. Chakraborty, and A. K. Singh, “A study on TEC reduction during the tail phase of the 21st June 2020 annular solar eclipse,” *Advances in Space Research*, vol. 67, no. 6, pp. 1948–1957, 2021.
- [4] D. Pundhir, B. Singh, and R. Singh, “Statistical and wavelet transform-based study of the latitudinal ionospheric response to an annular solar eclipse on June 21, 2020,” *Izvestiya-Atmospheric and Oceanic Physics*, vol. 58, no. 6, pp. 625–634, 2022.
- [5] S. Chakraborty, S. Palit, S. Ray, and S. K. Chakrabarti, “Modeling of the lower ionospheric response and VLF signal modulation during a total solar eclipse using ionospheric chemistry and LWPC,” *Astrophysics and Space Science*, vol. 361, no. 2, p. 72, 2016.
- [6] S. Kundu, S. Chowdhury, S. Palit, S. K. Mondal, and S. Sasmal, “Variation of ionospheric plasma density during the annular solar eclipse on December 26, 2019,” *Astrophysics and Space Science*, vol. 367, no. 5, p. 44, 2022.
- [7] C. H. Chen, C. C. H. Lin, C. J. Lee, J. Y. Liu, and A. Saito, “Ionospheric responses on the 21 August 2017 solar eclipse by using three-dimensional GNSS tomography,” *Earth Planets and Space*, vol. 74, no. 1, p. 173, 2022.
- [8] C. H. Chen, C. H. C. Lin, and T. Matsuo, “Ionospheric responses to the 21 August 2017 solar eclipse by using data assimilation approach,” *Progress in Earth and Planetary Science*, vol. 6, no. 1, p. 13, 2019.
- [9] A. Meza, G. Bosch, M. P. Natali, and B. Eylonstein, “Ionospheric and geomagnetic response to the total solar eclipse on 21 August 2017,” *Advances in Space Research*, vol. 69, no. 1, pp. 16–25, 2022.
- [10] P. Tiwari, N. Parihar, A. Dube, R. Singh, and S. Sripathi, “Abnormal behaviour of sporadic E-layer during the total solar eclipse of 22 July 2009 near the crest of EIA over India,” *Advances in Space Research*, vol. 64, no. 10, pp. 2145–2153, 2019.
- [11] E. L. Afraimovich, K. S. Palamartchouk, N. P. Perevalova, V. V. Chernukhov, A. V. Lukhnev, and V. T. Zalutsky, “Ionospheric effects of the solar eclipse of March 9, 1997, as deduced from GPS data,” *Geophysical Research Letters*, vol. 25, no. 4, pp. 465–468, 1998.
- [12] J. B. Habarulema, L.-A. McKinnell, and P. J. Cilliers, “Prediction of global positioning system total electron content using Neural Networks over South Africa,” *Journal of Atmospheric and Solar-Terrestrial Physics*, vol. 69, no. 15, pp. 1842–1850, 2007.
- [13] S. Sahu, R. Trivedi, R. K. Choudhary, A. Jain, and S. Jain, “Prediction of total electron content (TEC) using neural network over anomaly crest region bhopal,” *Advances in Space Research*, vol. 68, no. 7, pp. 2919–2929, 2021.
- [14] L. Liu, S. Zou, Y. Yao, and Z. Wang, “Forecasting global ionospheric TEC using deep learning approach,” *Space Weather*, vol. 18, no. 11, 2020.
- [15] K. D. Reddybattula, L. S. Nelapudi, M. Moses et al., “Ionospheric TEC forecasting over an Indian low latitude location using long short-term memory (LSTM) deep learning network,” *Universe*, vol. 8, no. 11, p. 562, 2022.
- [16] M. C. Iban and E. Şentürk, “Machine learning regression models for prediction of multiple ionospheric parameters,” *Advances in Space Research*, vol. 69, no. 3, pp. 1319–1334, 2022.
- [17] S. K. Chakrabarti, S. Sasmal, S. Chakraborty, T. Basak, and R. L. Tucker, “Modeling D-region ionospheric response of the Great American TSE of August 21, 2017 from VLF signal perturbation,” *Advances in Space Research*, vol. 62, no. 3, pp. 651–661, 2018.
- [18] S. Kiruthiga, S. Mythili, R. Mukesh, M. Vijay, and D. Venkata Ratnam, “Analysis of TEC values predicted by OKSM amongst low, mid and high latitude GPS stations during X 9.3 solar flare,” *Astrophysics and Space Science*, vol. 366, no. 8, p. 80, 2021.
- [19] R. Mukesh, V. Karthikeyan, P. Soma, and P. Sindhu, “Ordinary kriging-and cokriging-based surrogate model for ionospheric TEC prediction using NavIC/GPS data,” *Acta Geophysica*, vol. 68, no. 5, pp. 1529–1547, 2020.
- [20] S. Kiruthiga, S. Mythili, R. Mukesh, and S. C. Dass, “Prediction of ionospheric TEC during the annular and total solar eclipses that occurred over Indonesia by using OKSM and FFNN,” *Cosmic Research*, vol. 61, no. 6, pp. 471–486, 2023.
- [21] A. Tebabal, S. M. Radicella, B. Damtie, Y. Migoya-Orue, M. Nigussie, and B. Nava, “Feed forward neural network based ionospheric model for the East African region,” *Journal of Atmospheric and Solar-Terrestrial Physics*, vol. 191, 2019.
- [22] D. Salinas, V. Flunkert, J. Gasthaus, and T. Januschowski, “DeepAR: probabilistic forecasting with autoregressive recurrent networks,” *International Journal of Forecasting*, vol. 36, no. 3, pp. 1181–1191, 2020.
- [23] E. Şentürk, M. Saqib, and M. A. Adil, “A Multi-Network based Hybrid LSTM model for ionospheric anomaly detection: a case study of the Mw 7.8 Nepal earthquake,” *Advances in Space Research*, vol. 70, no. 2, pp. 440–455, 2022.
- [24] M. Saqib, E. Şentürk, S. A. Sahu, and M. A. Adil, “Comparisons of autoregressive integrated moving average (ARIMA) and long short term memory (LSTM) network models for ionospheric anomalies detection: a study on Haiti (Mw = 7.0) earthquake,” *Acta Geodaetica et Geophysica*, vol. 57, no. 1, pp. 195–213, 2022.
- [25] E. Şentürk, M. Arqim Adil, and M. Saqib, “Ionospheric total electron content response to annular solar eclipse on June 21, 2020,” *Advances in Space Research*, vol. 67, no. 6, pp. 1937–1947, 2021.